24th COBEM - 2017

24th ABCM International Congress of Mechanical Engineering
December 3-8, 2017, Curitiba, PR, Brazil

COBEM-2017-1040
MATHEMATIC MODELLING OF A SHAPE MEMORY ALLOY ACTUATOR

Matheus Paris Orsi[1]
Gustavo Luiz Chagas Manhães de Abreu[2]
São Paulo State University - UNESP, Faculdade de Engenharia de Ilha Solteira, Department of Mechanical Engineering, Av. Brasil, Centro, Ilha Solteira-SP, Brasil
[1]matheusorsi@gmail.com, [2]gustavo@dem.feis.unesp.br

Rafael de Oliveira Silva
University of Rio Verde - UniRV, Faculdade de Engenharia Mecânica, Fazenda Fontes do Saber, Caixa Postal 104, Rio Verde-GO, Brasil
rafa_engemec@hotmail.com

Abstract. *Shape Memory Alloys (SMAs) are materials capable of converting thermal energy into mechanical energy. Onde deformed permanently, these materials can return to their original shape through heating. SMA actuators present a potential alternative to the conventional ones due to its silent and clean atuation, but their response time is high. Several models were created to study characterize the thermomechanic behavior of an SMA. This paper aims to model an actuator of shape memory alloy and investigate two constitutive models of SMA in the scientific literature.*

Keywords: *Shape Memory Alloy (SMA), constitutive models, phase transformations, numerical analysis*

1. INTRODUCTION

Shape Memory Alloys (SMAs) are synthetic materials that have the property of recovering from inelastic strains (about 10%) or develop considerable forces of restitution while restraining it's recuperation, due to induced phase transformations (Paiva, 2004). Generally, SMAs can be easily deformed in a apparently plastic way at a low temperature and, when exposed to a field of temperatures, return to their original shape.

Shape memory alloys usually present low resistance to fatigue when compared to carbon steels. To improve this characteristic, several studies have been developed to analyze the effects of adding and combining certain alloy elements. SMAs present also low response time. Therefore, in situations where it is needed a fast response, other inteligent materials are recommended, such as piezoelectrics, which may produce more satisfatory results. However, it is important to highlight that that shape memory alloys are capable of generating great forces of restitution with a relatively low consume of energy (Wu and Schetky, 2000).

The development of SMA actuators present many atractives to various fields of engineering, mainly in robotics (Wu and Schetky, 2000; Ashrafiuon *et al.*, 2006), substituting the conventional actuators, which are heavy and noisy, like motors and solenoid valves. Shape memory alloy actuators possess the greater relation of useful load per actuator's weight in comparison to the conventional actuators, but, in some practical cases, SMA actuators are considered to be insufficient due to the elevated response time. For a fast actuation, the alloy must be heated to cause the contraction and cool it on recuperation. The heating process is simple and fast, and can be made with the passage of a electric current through the wire (Leo, 2007). On the other hand, the cooling process can be done by means of the instalation of a forced heat dissipation system (Romano and Tannuri, 2009).

Several models are proposed on the literature to replicate the nonlinear behaviour of these materials. This paper focuses on Gao's and Ikuta's models, comparing the martensitic fractions during phase transformations, to verify the influence of mechanic stress in each constitutive model for an Ni-Ti SMA.

2. IKUTA'S MODEL

According to Ikuta *et al.* (1991), the martensitic fraction is an exponencial function where phase transformations depend on the temperature only. There are two basic equations to describe the behaviour of an SMA. The first one refers to the heating process, where the transformation occurs from martensite to austenite, and the second refers to the cooling

of the SMA, occuring transformation form austenite to martensite:

$$\xi_h = \frac{\xi_M}{1 + \exp\left[\frac{6.2}{A_f - A_s}\left(T - \frac{A_f + A_s}{2}\right)\right]} \tag{1}$$

$$\xi_c = \frac{1 - \xi_A}{1 + \exp\left[\frac{6.2}{M_s - M_f}\left(T - \frac{M_f + M_s}{2}\right)\right]} + \xi_A \tag{2}$$

where ξ_h and ξ_c are the martensitic fractions of the SMA during heating and cooling, respectively; A_s is the start temperature of transformation to austenite; A_f is the final temperature of transformation to austenite; M_s is the start temperature of transformation to martensite; M_f is the final temperature of transformation to martensite; ξ_M and ξ_A correspond to, respectively, the martensitic fractions at the beginning of heating and cooling; T is the material's temperature and exp is the exponential function.

3. GAO'S MODEL

In Gao's model , the martensitic fraction is divided in two parts, induced by tension (ξ_s) and by temperature (ξ_t) (Gao *et al.*, 2007). Therefore, the total martensitic fraction is:

$$\xi = \xi_s + \xi_t \tag{3}$$

Studies performed by Brinson (1993) point out a dependance of Young's modulus (Y) related to the total martensitic fraction. To account for this dependance, a simple linear function is chosen:

$$Y(\xi) = Y_A + \xi(Y_A - Y_M) \tag{4}$$

where Y_A is the Young's modulus for austenite phase and Y_M is the Young's modulus corresponding to martensite phase.

The transformations' regions are described by the diagram on Figure 1. M_s, M_f, A_s and A_f are the same temperatures described in Ikuta's model.

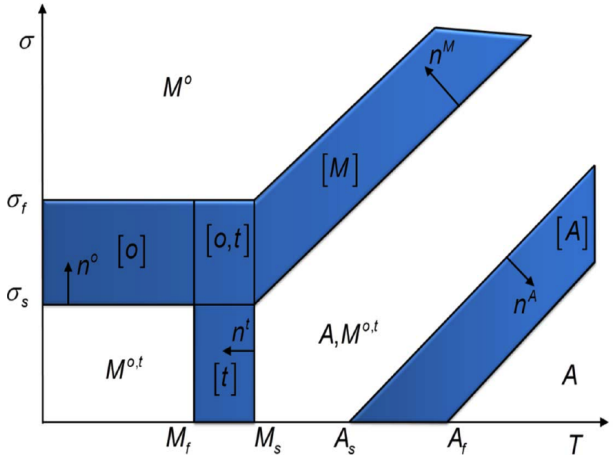

Figure 1. Phases diagram according to Gao's model

The blue sections on Fig. 1 are the transformations regions, while the white parts are called ``Dead Zones´´, where there is not transformation. The transformation regions are:

- $[A]$: Transformation from martensite to austenite;
- $[M]$: Transformation from twinned martensite and/or austenite to detwinned martensite.
- $[o]$: Transformation from twinned martensite to detwinned martensite
- $[t]$: Transformation from austenite to twinned martensite.

Every region of transformation has a transformation vector. It means that the conversion between phases will only occur if the thermomechanic loading present a positive component on the direction of the region's vector. That is, the transformation will happen if:

$$\tau^i \cdot n^i > 0 \qquad i = [M], [A], [o], [t] \tag{5}$$

where τ is the tangent vector to the loading's path and i represents the region of transformation.

To verify whether the transformation happens, it is required to know the transformatin vectors' components in coordinates σ and T. Table 1 shows the calculus of the components. n_1^i and n_2^i represents the vector's component in temperature (T) and tension (σ) coordinates, respectively. It also contains the entrance (T_{in}^i, σ_{in}^i) and exit ($T_{out}^i, \sigma_{out}^i$) points of transformation zones.

Table 1. Components of transformation vectors and poins of entrance and exit for each transformation zone

Region	$(T_{in}^i, \sigma_{in}^i)$	(n_1^i, n_2^i)	$(T_{out}^i, \sigma_{out}^i)$
[M]	(M_s, σ_s)	$\frac{C_M}{\sqrt{1+C_M^2}}, \frac{1}{\sqrt{1+C_M^2}}$	(M_s, σ_f)
[A]	$(A_s, 0)$	$\frac{C_A}{\sqrt{1+C_A^2}}, \frac{-1}{\sqrt{1+C_A^2}}$	$(A_f, 0)$
[t]	$(M_s, 0)$	$(-1, 0)$	$(M_f, 0)$
[o]	(M_s, σ_s)	$\frac{C_D}{\sqrt{1+C_D^2}}, \frac{1}{\sqrt{1+C_D^2}}$	(M_s, σ_f)

The coefficient C_D in Table 1 indicates the inclination of region [o], which is considered to be zero in this paper. With that, region [o] remains in horizontal position.

Eqs. 6 to 13 describe the evolution of martensitic fraction during transformation. The index "swi" refers to the last switch point during transformation.

$$\xi_t^{[A]} = \xi_t^{swi}\left[\frac{1}{2} + \frac{1}{2}\cos\left(\pi Z^{[A]}\right)\right] \tag{6}$$

$$\xi_s^{[A]} = \xi_s^{swi}\left[\frac{1}{2} + \frac{1}{2}\cos\left(\pi Z^{[A]}\right)\right] \tag{7}$$

$$\xi_t^{[A]} = 1 - \xi_s^{swi} - (1 - \xi_s^{swi} - \xi_t^{swi})\left[\frac{1}{2} + \frac{1}{2}\cos\left(\pi Z^{[t]}\right)\right] \tag{8}$$

$$\xi_s^{[t]} = \xi_s^{swi} \tag{9}$$

$$\xi_t^{[M]} = \xi_t^{swi}\left[\frac{1}{2} + \frac{1}{2}\cos\left(\pi Z^{[M]}\right)\right] \tag{10}$$

$$\xi_s^{[M]} = \xi_s^{swi} + (1 - \xi_s^{swi})\left[\frac{1}{2} + \frac{1}{2}\cos\left(\pi Z^{[M]}\right)\right] \tag{11}$$

$$\xi_t^{[o]} = \xi_t^{swi}\left[\frac{1}{2} + \frac{1}{2}\cos\left(\pi Z^{[o]}\right)\right] \tag{12}$$

$$\xi_s^{[o]} = \xi_s^{swi} + (1 - \xi_s^{swi})\left[\frac{1}{2} + \frac{1}{2}\cos\left(\pi Z^{[o]}\right)\right] \tag{13}$$

The factor Z^i is given by:

$$Z^i(T, \sigma) = \frac{\rho^i - \rho_j^i}{\rho_0^i - \rho_j^i} \tag{14}$$

where ρ^i, ρ_j^i, ρ_0^i and ρ_j^i are relative distances to the present point of SMA inside transformation zones. Fig. 2 shows an example for zone [M].

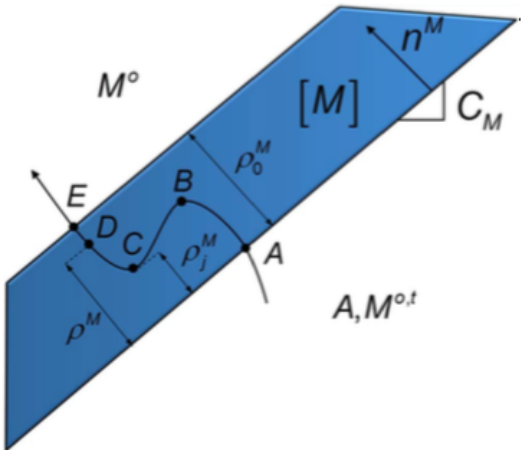

Figure 2. Relative distances ρ inside zone [M]

4. COMPARISON BETWEEN GAO AND IKUTA'S MODELS

The material chosen for computational simulations was a Nickel-Titanium SMA with properties listed in Table 2.

Table 2. Properties of Ni-Ti Shape Memory Alloy

Young's Modulus	**Temperatures of Transformation**	**Constants of Transformation**
$Y_A = 67 \times 10^3 MPa$	$M_f = 9\,°\text{C}$	$C_M = 8MPa\,°\text{C}^{-1}$
$Y_M = 26.3 \times 10^3 MPa$	$M_s = 18.4\,°\text{C}$	$C_A = 13.8MPa\,°\text{C}^{-1}$
Maximum Residual Deformation	$A_s = 34.5\,°\text{C}$	$\sigma_s = 100MPa$
$\varepsilon_L = 0.032$	$A_f = 49\,°\text{C}$	$\sigma_f = 170MPa$

For an effective comparison, it has been simulated three heating thermomechanical loadings and other three to the cooling process. Varying the temperature from -20°C to 100 °C (heating), and from 100°C to -20°C (cooling) the martensitic fractions were computed for different constant values of mechanic stresses.

On heating, it has been applied values of mechanic stress of $10MPa$, $100MPa$ and $200MPa$. Obtained curves of martensitic fraction as a function of temperature are shown on Fig. 3(a).

On cooling process, similar thermomechanical loadings have been applied also on Gao's model. However, the new values were $10MPa$, $170MPa$ and $171MPa$. Analogically to heating process, the curves of martensitic fraction as a function of temperature are presented on Fig. 3(b).

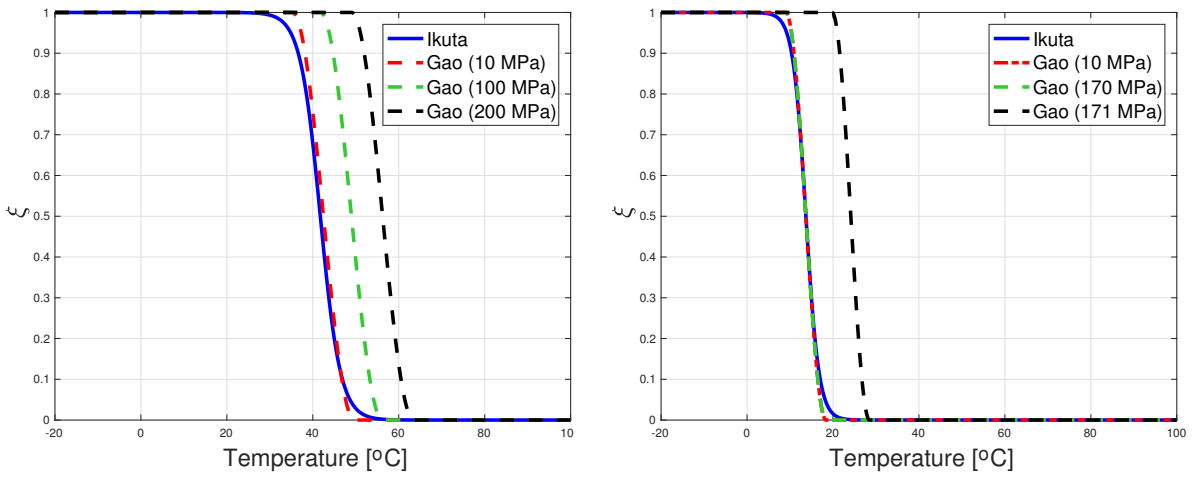

(a) (b)

Figure 3. Evolution of ξ during (a) heating and (b) cooling

Fig. 3(a) shows that the higher the value of mechanic stress applied to the alloy, the bigger the difference between both models. In addition, before the phase transformation is completed (martensite or austenite), the martensitic fraction

maintains 1 when the material is composed by pure martensite, or 0 when it is composed by pure austenite and, during the transformations, the martensitic fraction varies following an exponential function.

As seen on Fig. 3(b), values of mechanic stress below the critic point ($170MPa$) on Gao's model produce a very similar curve of ξ to Ikuta's model. However, values above the critic point tend to create more distant curves between both models.

5. EXPERIMENTAL RESULTS

To validate the presented models, it has been built an actuator of SMA wire with $0.5mm$ of diameter, with initial and final lengths of $230mm$ and $270mm$, respectively. Fig. 4 shows the experimental apparatus.

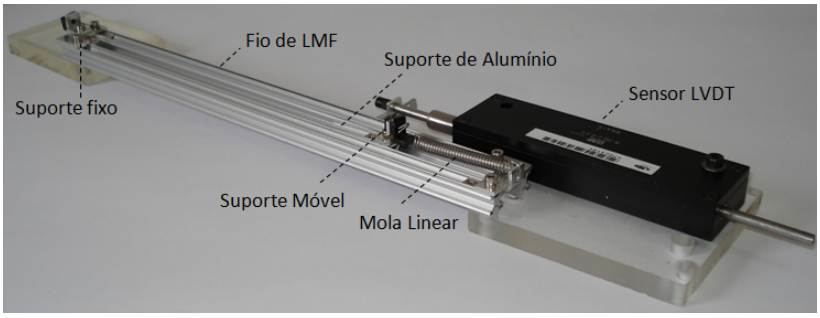

Figure 4. SMA actuator built

It has been used an SMA made by *NiTinol*, attached to an aluminum structure and to a mobile support. Between the extremities of the wire, it has been connected a power source, to promote the heating or cooling of the wire. Also, it has been connected a position sensor to verify the wire's displacement.

5.1 ACTUATOR'S DYNAMIC MODEL

Considering the actuator may be modelled as a system with one degree of freedom, it can be ilustrated by:

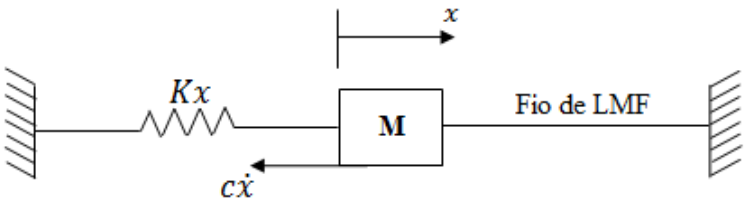

Figure 5. SMA actuator's scheme

where M is the mass of the mobile support, c is the friction's coefficient between the mobile support and the linear guide, K is the linear coil's stiffness and F_{SMA} is the force over the SMA wire.

From Second Newton's Law, the movement's equation of the system is:

$$M\ddot{x} + c\dot{x} + Kx = F_{SMA} \tag{15}$$

Considering the SMA as a coil with stiffnes K_{SMA}, the force F_{SMA} was calculated, assuming that:

- On austenite phase, the wire's length is L_0;
- On martensite, the wire's length is L_f, corresponding to the actuator's position $x = 0$;
- On and intermediary phase, the displacement of the wire is given by $\Delta L = \epsilon_f L_f - x$, with ϵ_L being the maximum residual deformation.

Fig. 6 ilustrates the assumptions.

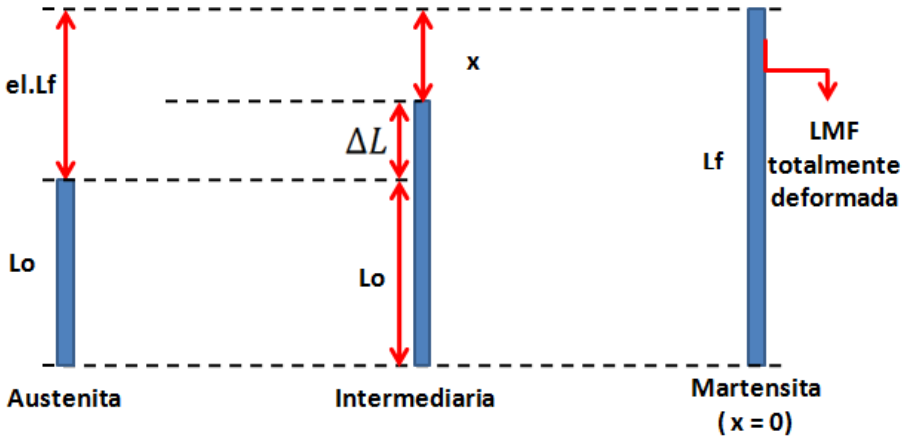

Figure 6. Behaviour of SMA's wire

From Hooke's Law:

$$F_{SMA} = K_{SMA}\Delta L = K_{SMA}(\epsilon_L L_f - x) \tag{16}$$

where x is the position of the actuator.

To calculate K_{SMA} as a function o martensite fraction (ξ), the mechanic stress if considered to be:

$$\sigma = \xi\epsilon Y_M + (1-\xi)\epsilon Y_A \tag{17}$$

where Y_M and Y_A are the Young's modulus for martensite and austenite, respectively and ϵ is the displacement of the wire.

Assuming $Y_A >> Y_M$:

$$\sigma = (1-\xi)\epsilon Y_A \tag{18}$$

Substituting $\epsilon = \frac{\Delta L}{L_0}$ e $\sigma = \frac{F_{SMA}}{A}$:

$$\frac{F_{SMA}}{A} = (1-\xi)Y_A\frac{A}{L_0} \tag{19}$$

By analogy to Hooke's Law (Eq. 16), the non linear coil's stiffness of a SMA wire is given by:

$$K_{SMA} = (1-\xi)Y_A\frac{A}{L_0} \tag{20}$$

Therefore, the movement's equation is rewritten by:

$$M\ddot{x} + c\dot{x} + (K + K_{SMA})x = K_{SMA}\epsilon_L L_f \tag{21}$$

5.2 THERMAL MODEL

A frequently used model that relates heat transfer with electrical heating of a wire (*Joule effect*) is given by (Leo, 2007):

$$(\rho A)C_p\frac{dT(t)}{dt} = I^2 R_w - h_q A_c[T(t) - T_\infty] \tag{22}$$

where ρ is the mass density of the SMA; A is the transversal section area; C_p is the specific heat of the SMA wire; R_w is the electric resistance by unit of length; h_q is the coefficient of heat transfer by convection; A_c is the area of heat exchange per unit of lenght; T_∞ is the enviroment's temperature and I is the applied electric current.

An SMA wire's electric resistance may be considered to be analogue to a convecional conductive wire, or:

$$R_{eq} = \rho_{el}\frac{L}{A} \tag{23}$$

where R_{eq} is the wire's electric resistance, ρ_{el} is the material's resistivity, A is the transversal section's area and L is the wire's length.

With basis on Eq. 23, the electric resistance of the SMA wire, per unit of length, is given by:

$$R_w = \frac{\rho_{el}}{A} \tag{24}$$

According to Gil and Planell (1998), Shape Memory Alloys' physical properties change with the crystaline structure present on the material. Because of that, Elahinia and Ahmadian (2005) and Garner *et al.* (2000) proposed the utilisation of Eq. 4 to describe the variation of electric resistivity with martensitic fraction ξ, where it is possible to notice a similarity with the equation of Young's modulus of (Brinson, 1993).

$$\rho_{el} = \rho_{el_A} + \xi(\rho_{el_M} - \rho_{el_A}) \tag{25}$$

where ρ_{el} is the total resistivity of the material and ρ_{el_M} and ρ_{el_A} are the resistivities on phases martensite and austenite, respectively.

In this paper, the same principle is used to describe the specific heat as a function of ξ. As an analogy to Brinson (1993), the specific heat is given by:

$$C_p = C_{pA} + \xi(C_{pM} - C_{pA}) \tag{26}$$

with C_{pM} and C_{pA} being, respectively, the specific heat on phases martensite and austenite.

The coefficient of heat transfer by convection (h) depends mainly on the temperatures' difference between the material and the work fluid and on the geometry of the body. One of the estimations for the value of h is given by (Holman, 1999):

$$h = 1.32 \left[\left(\frac{T_{op} - T_\infty}{d} \right)^{\frac{1}{4}} \right] \tag{27}$$

where T_{op} is the operation temperature of the SMA wire in °C, h_q is the coefficient of heat transfer by convection in $W/m^2 \cdot^\circ$ C and d is the diameter of the SMA wire in meters.

5.3 POWER SUPPLY

To control the temperature of the SMA, it was utilized a controllable power source (model Lord RD-3002-1), with currents from $0A$ to $2A$, through the imposition of entrance values of tension from $0V$ to $5V$. The power source, according to it's manufacturer, provided the following relation between current (I) and electric tension (u):

$$I = 0.4643(u - 0,6) \tag{28}$$

5.4 VALIDATION OF THE ACTUATOR'S MODEL

Firstly, a series of parameters were stablished for the actuator, such as A_s, A_f, M_s, M_f, coefficients of heat transfer by convection, among others, as shown in Table 3.

Parameter	Unit	Initial Value
M_f	°C	40.00
M_s	°C	50.00
A_s	°C	55.00
A_f	°C	70.00
C_p	$\frac{J}{kg \cdot^\circ \mathrm{C}}$	857.00
c	$\frac{N \cdot s}{m}$	0.02
ρ_{el_M}	$\mu\Omega \cdot m$	0.76
ρ_{el_A}	$\mu\Omega \cdot m$	0.82
h_h	$\frac{w}{m^2 \cdot^\circ \mathrm{C}}$	16.43
h_c	$\frac{w}{m^2 \cdot^\circ \mathrm{C}}$	22.47

Table 3. Initial parameters

The ambient temperature was measured with a conventional termometer and it was found that $T_\infty = 28°$C. Coefficients of heat exchange by convection were calculated by Eq. 27.

It proceeded, then, to the experiments. The electric tension entrance on the actuator is ilustrated on Fig. 7(a). The first obtained experimental curve of displacement as a function of time is shown in Fig. 7(b)

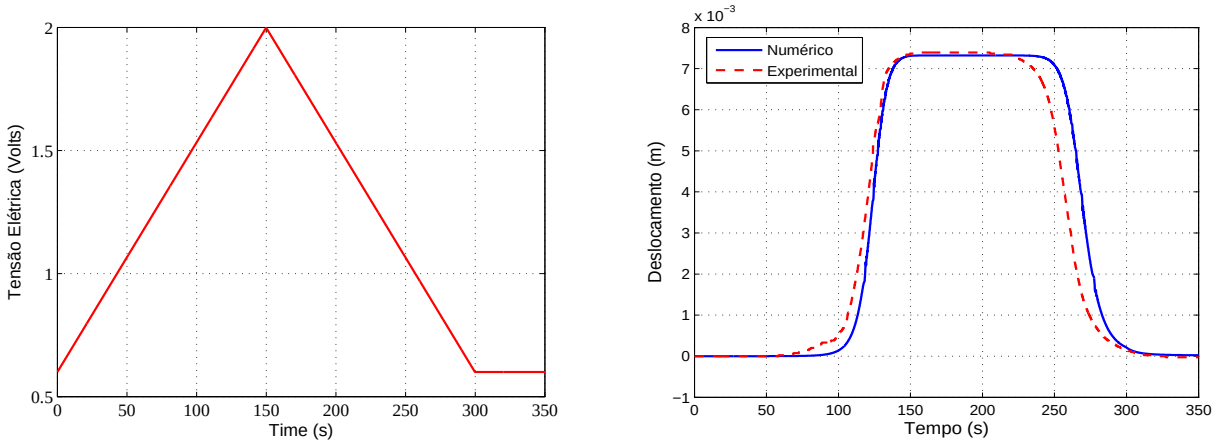

(a) Stablished entrance signal for electric tension (u)

(b) Initial curves obtained experimentally

Figure 7. Initial test on the actuator

It is seen that the difference between numeric and experimental curves can not be disconsidered. Because of that, it became necessary an optimization of parameters to approximate both curves. For that, it was used the *Matlab*® function *fmincon*. Table 4 shows the parameters after the optimization and Fig. 8(a) shows the curves with the new values.

Parameter	**Unit**	**Final**
M_f	^oC	$39,76$
M_s	^oC	$51,14$
A_s	^oC	$53,91$
A_f	^oC	70.76
C_{p_M}	$J/kg.^oC$	$855,19$
C_{p_A}	$J/kg.^oC$	$856,51$
c	$\frac{Ns}{m}$	$0,89$
ρ_{el_M}	$\mu\Omega.m$	$0,78$
ρ_{el_A}	$\mu\Omega.m$	$0,80$
h_h	$W/m^2.^oC$	$16,91$
h_c	$W/m^2.^oC$	$26,69$

Table 4. Optimized parameters for the actuator

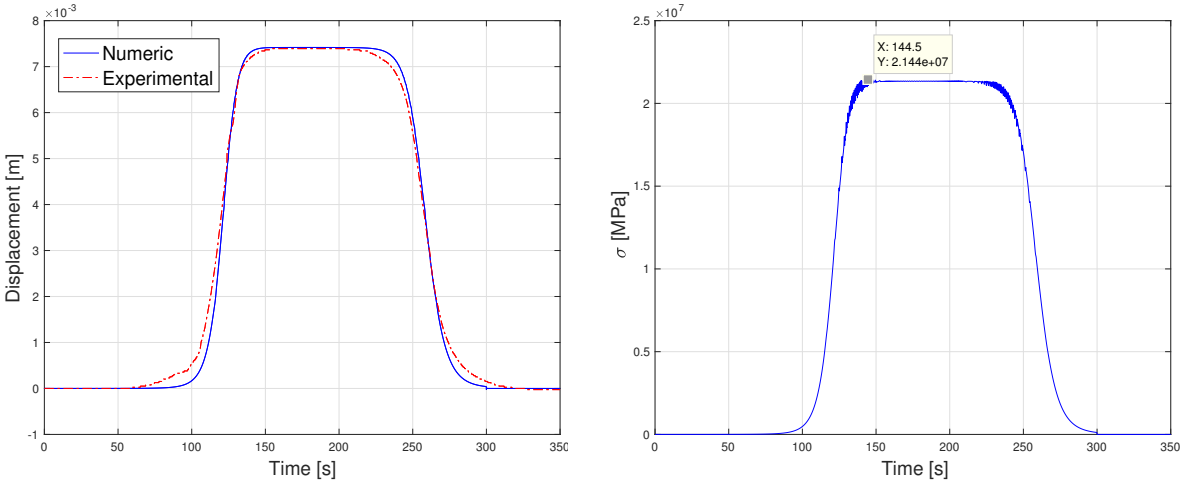

(a) Curves after optimization

(b) Evolution of mechanic stress over time

Figure 8. Final tests

Scanning the values of displacement on Fig. 8(a) and transforming it into values of mechanical force according to the actuator's dynamic model, the stress in each point of the experiment was obtained by:

$$\sigma = \frac{F_{SMA}}{A} \tag{29}$$

where A is the area of the transversal section of the SMA wire, given by:

$$A = \frac{\pi \cdot d^2}{4} = \frac{pi \cdot (0,5 \times 10^{-3})^2}{4} = 1.963 \times 10^{-7}\ m^2 \tag{30}$$

Calculating the stress for each point of the curve, it was built the chart on Fig. 8(b). The highlited point is the maximum value of mechanic stress on the alloy during the experiments.

Therefore, the maximum mechanic stress encountered was $21.44MPa$. Using this value on Gao's model and comparing both models once again, it was verified the possibility to use Ikuta's model to study the actuator because, as seen in section 1, this model is substantially simpler for numerical implementations. Fig. 9 contains the evolution of ξ during a cycle of heating and cooling under the mentioned value of stress.

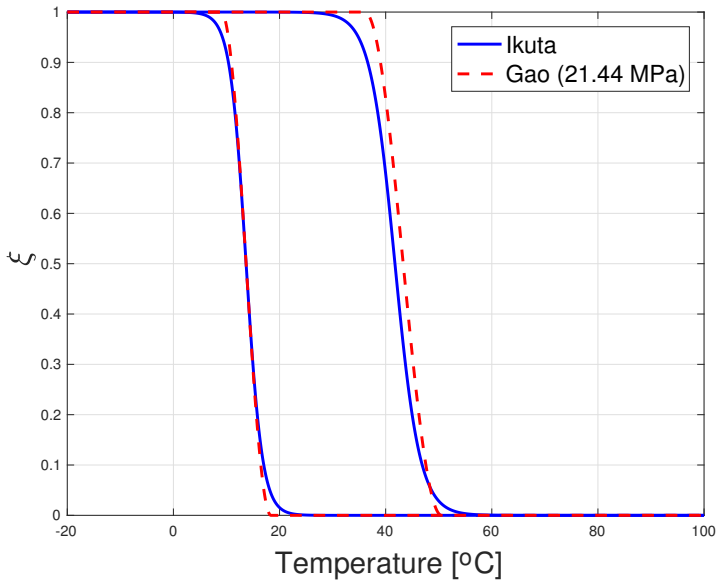

Figure 9. Evolution of ξ during a cycle of temperatures

The chart shows that the largest difference is found at heating, as it was mentioned before. However, curves of both models are very similar in general.

6. CONCLUSIONS

This paper presents the modelling of a shape memory alloy actuator and a comparation between two constitutive models of the literature, verifying the possibility of utilization of Ikuta's model to describe phase transformations.

The effects of phase cheanges were experimentally verified using a controlable power source, with a ramp entrance. The test was performed to adjust the parameters utilized on the model constructed in comparation to experimental results. After the optimization of parameters, the computational model was proven to be valid to describe the behaviour of the Ni-Ti SMA, showing a good compliance between experimental and numeric results.

From Figs. 3(a) and 3(b), it is possible to conclude that, for values of stress of up to $30MPa$ on heating and $170MPa$ on cooling, it is possible to use Ikuta's model to describe an SMA behaviour. Based on this conclusion, from Figs. 8(b) and 9, it is shown that, for the studied prototype, the utilization of Ikuta's model on computational procedures is justifiable. This is an excellent alternative, due to the high level of complexity of Gao's model and the simplicity of Ikuta's model.

7. ACKNOWLEDGEMENTS

The authors would like to thank the FAPESP (Process 2016/05660-7) for the financial support of the reported research.

8. REFERENCES

Ashrafiuon, H., Eshraghi, M. and Elahinia, M.H., 2006. "Position control of a three-link shape memory alloy actuated robot". *Intelligent Material Systems and Structures*, Vol. 17, pp. 381–392.

Brinson, L.C., 1993. "One-dimensional constitutive behavior of shape memory alloys: Thermamechanical derivation with non-constant material functions and redefined martensite internal variable". *Smart Materials and Structures*, Vol. 4, pp. 229–242.

Elahinia, M.H. and Ahmadian, M., 2005. "An enhanced sma phenomenological model: Ii. the experimental study". *Smart Material and Structures*, Vol. 14, pp. 1309–1319.

Gao, X., Qiao, R. and Brinson, L.C., 2007. "Phase diagram kinetics for shape memory alloys: A robust finite element implementation." *Smart Materials and Structures*, Vol. 16, pp. 2102–2115.

Garner, L.J., Wison, L.N., Lagoudas, D.C. and Rediniotis, K., 2000. "Development of a shape memory alloy actuated biomimetic vehicle". *Smart Material and Structures*, Vol. 9, pp. 673–683.

Gil, F.J. and Planell, J.A., 1998. "Shape memory alloys for medical applications". *journal of Engineering in Medicine*, Vol. 212 Part H, pp. 473–488.

Holman, J.P., 1999. *Heat Transfer*. McGraw Hill, 10th edition.

Ikuta, K., Tsukamoto, M. and Hirose, S., 1991. "Mathematical model and experimental verification of shape memory alloy for designing micro actuator." *Proceedings of the IEEE on micro electromechanical systems, an investigation of microstructures, sensors, actuators, machines, and robots*, pp. 103–108.

Leo, D., 2007. *Heat Transfer*. John Willey and Sons.

Paiva, A., 2004. *Modelling of thermomechanic behaviour of shape memory alloys*. Ph.D. thesis, Department of Mechanical Engineering, Pontificia Universidade Católica, Rio de Janeiro.

Romano, R. and Tannuri, E., 2009. "Modeling, control and experimental validation of a novel actuator based on shape memory alloys". *Mechatronics*, Vol. 19, pp. 1169–1177.

Wu, M.H. and Schetky, L.M., 2000. "Industrial applications for shape memory alloys". *Pacific Groove, California*, pp. 171–182.

9. RESPONSIBILITY NOTICE

The authors are the only responsible for the printed material included in this paper.